CrossMark

Influences of coal mines, metallurgical plants, urbanization and lithology on the elemental composition of street dust

Gorazd Žibret [iD]

Abstract Street dust (SD) acts as a sink and a source of atmospheric particulate matter, which is especially significant in urban environments. World studies of natural and anthropogenic impacts on the elemental composition of SD are generally limited to specific areas or case studies. The objectives of this study are to determine the impacts of different anthropogenic atmospheric dust emitters and natural factors on the chemical composition of SD, and to define sources of variance in elemental composition of SD, temporal variations and geochemical associations of elements on large number of samples, collected in different time periods, anthropogenic environments and geological settings. Nested ANOVA shows that the majority of the elemental-level variations were found to be regional ones. Increased variations on local scale were observed for Hg, Mo, Ni, Zn and Ag. Increased temporal variations were observed for Zn, As, Cd and Pb. Spatial variations within the same sampling location were increased for Hg and Ag. Three anthropogenic geochemical associations were detected: Coal mining and coal-fired power production enriched SD with Al, Co, Fe, La, Sc, Th, Ti, V, Zr and U, metallurgy with Cr, V, Ni and Mn, and urbanization with Ag, Bi, Ca, Cd, Mg, Mo, Pb and Zn.

Introduction

Street dust (SD) is a complex mixture of particles of natural and anthropogenic origin. Sources of natural particles are soil dusting, sea salt, volcanic ash, pollen, plant remains and forest fires (Bernabe et al. 2005). Anthropogenic particles originate from the domestic heating, weathering of construction materials, traffic (wear of brake pads and tires, fuel combustion, catalytic converters), high-temperature industrial combustion processes (Piña et al. 2000; Bernabe et al. 2005; Li et al. 2016), past and present mining (Bavec et al. 2014; Bavec 2015) and metallurgical activities (Barandovski et al. 2008). Secondary aerosols, which form as a result of complex chemical and physical processes between natural and anthropogenic substances in the atmosphere, are also an important source of particles in SD (Venturini et al. 2014).

Traffic and industry are the largest sources of metals in SD in large cities (Wei et al. 2015). The wearing of brake pads produces particles containing Al, Si, S, Ti, Fe, Cu, Sb and Ba (Adachi and Tainosho 2004) and, according to the study of Amato et al.

G. Žibret (✉)
Geological Survey of Slovenia, Dimičeva ulica 14,
1000 Ljubljana, Slovenia
e-mail: gorazd.zibret@geo-zs.si

([2011](#)), Sb, Cu, Mo, Fe, Sn, Ba, Zr, Hf and Zn. Tire wear particles contain Zn, Mo, Cd, Ge and organic carbon, while exhaust particles contain organic carbon, Ni, Zn and Mo. Car paint can contain Si, Ca, Cr and Pb, while tire tread contains Al, Si, S, C and Zn (Adachi and Tainosho 2004). Traffic is also responsible for emissions of platinum group metals (Pt, Pd and Rh) which can be found in catalytic converters (Whiteley and Murray 2003; Prichard et al. 2009). The second important source of particles in SD of a large town is the abrasion of construction materials such as asphalt, concrete or natural stone (Kemppainen et al. 2003), emissions from demolition and construction activities, soil and plant remains, dusting and sea spray (the last one in the case of coastal areas; Amato et al. 2011). Industry can also be an important source of particles in SD (Manno et al. 2006; Tokalıoğlu and Kartal 2006; Al-Khashman 2007; Zheng et al. 2010). Even small-scale industrial activities can have a significant impact on the chemical composition of SD (Žibret and Rokavec 2010; Žibret 2012; Miler and Gosar 2015). Past environmental burdens can also influence the present SD composition (Charlesworth et al. 2003; Žibret 2012). The majority of the potential toxic metals in SD are found in the fraction < 125 μm (Herngren et al. 2006; Wang et al. 1998).

SD acts as a sink of atmospheric particulate matter in urban environments and can contain a high amount of different potentially toxic metals, while its remobilization by traffic, wind or improper street sweeping practices can act as a significant source of inhalable PM_{10} and $PM_{2.5}$ particles in the ambient air in urbanized environments (Amato et al. 2014). That is why contaminated SD may pose a health risk, especially to children (Shi et al. 2011), which can be even greater than that of traffic emissions (Zheng et al. 2010). Metals in SD can be chemically mobile and thus can easily enter the bloodstream if ingested (Tokalıoğlu and Kartal 2006). Cd and Zn from SD can easily be dissolved by rainwater, especially in acid rain conditions (Duong and Lee 2009), so the runoff water from urbanized areas can be highly toxic to aquatic organisms (Wang et al. 1998; McQueen et al. 2010; Watanabe et al. 2011).

SD is an important source, pathway and receptor of inhalable harmful particles in urban environments. A lot of scientific literature addresses the chemical composition of SD, the physical and chemical properties and sources of particles, natural and

anthropogenic factors which change the elemental composition of SD, as well as the impacts of contaminated SD on the environment and human health. However, majority of such studies were undertaken in the localized environments, on small number of samples. Only few consider samples taken far apart. Data analysis on larger datasets, as this is done for soils (Gosar et al. 2016), soils and sediments (Salminen et al. 2005) or moss (Harmens et al. 2010), is needed also for the SD.

Therefore, the objectives of this study are to define percentile distribution of 47 elements in SD, to determine the sources of variance, and to define geochemical associations of elements and impacts of natural and anthropogenic sources of atmospheric dust on the composition of SD. The significance of this research is that this study consider many samples, collected and analyzed by following the same procedures and methods, taken far apart, taken from the same areas as many as 15 years apart and collected on different geological and anthropogenic environments. In this way, results presented in this study do not show only local-scale variations and trends, but more global and generalized ones can be established.

Materials and methods

Description of the study areas

Data from four different sampling areas were collected (Table 1, Fig. 1). Each study area is characterized by one or more anthropogenic sources of atmospheric dust in the environment and by distinctive geo-environmental conditions.

The Slovenian (SLO) study area contains SD composition data from urbanized areas in Slovenia. Data were obtained from the study of Šajn (1999), where SD was collected in the five biggest Slovenian urbanized areas in 1996 (SLO), as well as from SD samples collected from the Slovenian capital, Ljubljana, in 2012. The Celje (CEL) study area is characterized by historical pollution caused by a 100-year Zn smelting chemical and metallurgical industry tradition and recent dust emissions from chemical factory, where the main product is Ti-based white pigment. The historical environmental burden in this area is approximately 12 × 9 km large Pb–Zn–Cd anomaly in soil, while chemical industry is a source of particles

Table 1 Description of the study areas where the elemental composition of SD was studied, with corresponding basic data and dominant sources of ambient dust and the sources of data

| Area	Location	Latitude	Longitude	Approx. area (km²)	No. of samples	Years of sampling	Potential anthropogenic sources	Detected anthropogenic atmospheric emission (based on observations of spatial distribution of elemental levels)	Geo-environment	Reference
SLO	Slovenian urban areas	45.5–46.5N	13.6–16.3E	50	26	1996 and 2012	Traffic, urbanization		Carbonates, clastites	Šajn (1999) and this study
CEL	Celje area, Slovenia	46.24N	15.27E	20	30	1996, 2005, 2009, 2012	Historical Pb–Zn–Cd pollution, ironworks, Ti white pigment factory, metal casting	Ti, Mn, Cr, Fe, Ni, Mo, Cu, Cr	Carbonates	Žibret and Rokavec (2010), Žibret (2012) and this study
SOK	Sokolov area, Czech Republic	50.2N	12.7E	150	113	2010, 2011, 2012	Coal mining, coal-fired power plant	Be, Li, Al, As	Metamorphic and clastic	This study
WIT	eMalahleni area, Republic of South Africa	25.85S	29.2E	700	137	2011, 2013	Coal mining, fly ash, smelting, traffic	V, Cr, Co, Fe, Mn, Al, Sr, Ba, Li	Clastites, paleozoic	Žibret et al. (2013) and this study
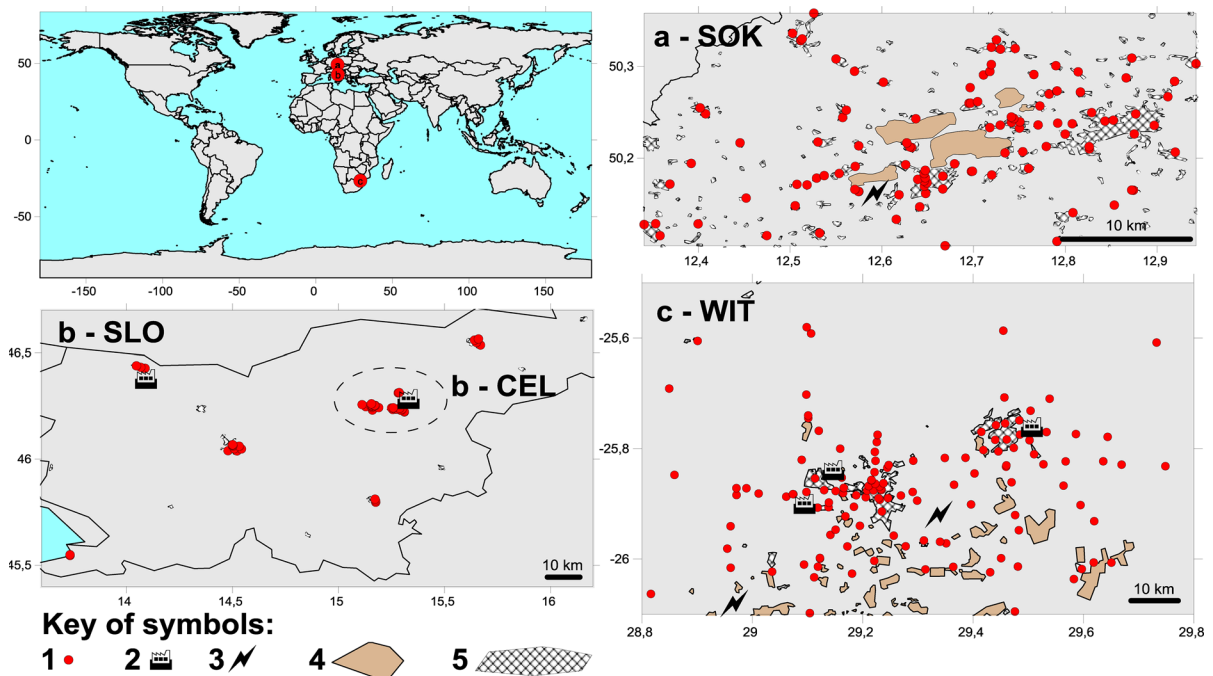
Fig. 1 Study areas. Key of symbols: 1—SD sampling point; 2—major metallurgical, smelting or casting plant; 3—large power plant; 4—coal mining areas; 5—villages and towns. **a** SOK—Sokolov (Czech Republic) study area; **b** SLO—Slovenian towns study area; **b** CEL—Celje study area; **c** WIT—eMalahleni (Republic of South Africa) study area

containing Ti and Nb (Šajn 2005; Žibret and Šajn 2008). A small bronze casting factory with localized impacts is also located in the nearby rural town of Žalec. The next area, located in the northwestern part of the Czech Republic near the town of Sokolov (SOK), is characterized by a 5 × 3 km large active open-pit lignite mine with adjacent coal-fired power plants and chemical industry. The eMalahleni area (formally known as Witbank town; WIT), approximately 100 km to the east of Johannesburg in the Republic of South Africa, is one of the most industrialized areas in Africa. The abundance of very easily accessible high-quality black coal caused numerous coal-fired power plants and large iron, chromium and vanadium smelters and casts being operating in the vicinity (Žibret et al. 2013).

Sampling procedure and chemical analysis

Sampling of the SD was conducted in warm part of the year after at least 7 successive days without precipitation on hard surfaces like asphalt or concrete. The sampling began with the removal of sand, stones and

other coarse material (free load) using a soft broom. This material was not sampled. Only fixed loads electrostatically connected within pores of asphalt or concrete (Vaze and Chiew 2002) were collected by brushing the asphalt or concrete surface. Special care was taken to avoid sampling of street dust in the areas of soil accumulation or vegetation remains. A composite sample weighing at least 250 g was collected at a minimum of 10 suitable paved surfaces in an area approximately 50 × 50 m around the sampling point, which location was pre-selected in areas containing larger paved surfaces (car parking lots, playgrounds, bridges, larger intersections or similar) from aerial photographs.

Pre-analytical preparation of the samples consisted of removing unwanted materials (stones, sand, plant remains, hair, textiles and similar) from the material of interest (fine-grained particles deposited from the atmosphere) by using 1 mm sieve. Samples were then air-dried in a ventilating oven at 303 K until a constant weight had been achieved. The drying temperature 303 K was selected to avoid Hg evaporation from samples (Adriano 1986). If particle

aggregates were present, they were gently crushed in a ceramic mortar. Because the highest levels of metals in road-deposited sediments in cities are found in the fine fraction of road dust, mostly in the size range < 0.125 mm (Wang et al. 1998; Herngren et al. 2006; Lanzerstorfer and Logiewa 2018), the samples were sieved using 0.125-mm sieve. 5 g of the material (< 0.125 mm) represented the material for the chemical analyses.

The samples were placed in small closed plastic containers and shipped to the commercial laboratory ACME Analytical Laboratories (Vancouver) Ltd., Canada (The company is now renamed to Bureau Veritas Mineral Laboratories). Forty-seven chemical elements were analyzed by inductively coupled plasma mass spectrometry (ICP-MS) following a four-acid digestion (a mixture of $HClO_4$, HNO_3, HCl and HF at 200 °C). The presence of Hg was determined by cold vapor atomic absorption spectrometry (AAS-CV) after aqua regia digestion (a mixture of HCl, HNO_3 and water at 95 °C). Where upper limit values were exceeded, four-acid digests were diluted by triple distilled water in a 1:9 ration and reanalyzed. To assure direct comparability of the results from different sampling campaigns, all samples were collected and processed by the same sampling procedure, and analyzed in the same laboratory using same analytical procedure.

Quality control

The following procedure assured the unbiased treatment of the samples and random distribution of a possible drift in the analytical conditions:

- samples were labeled with their laboratory ID numbers; the ID number contained no information regarding the material in the container;
- 10% of the randomly selected samples were shipped and analyzed in duplicates;
- geochemical standards were analyzed along with SD samples (OREAS24P, OREAS24E, OREAS45CA, DS8, DS9);
- an analysis of blank sample for every 20 analyzed samples was performed;
- samples were divided into two groups; the first group contained samples which were collected on the areas of no known pollution, while the second group contained samples where a high levels of

potential toxic metals were expected. The laboratory was instructed to initially analyze the first group and then the second group; and

- all samples within one group, replicates, bulk samples and geological standards were submitted to the laboratory in random order.

The measured quality control parameters of the chemical analyses are accuracy, measured with the recovery rate (%R, Eq. 1), precision, measured with the average relative percent difference (RPD, Eq. 2), and bias, measured by the average detected elemental levels in blank samples (BLN).

$$\%R = \frac{100}{n} \cdot \sum_{i=1}^{n} \left[1 + \left(\frac{Y_i - X_i}{X_i} \right) \right] \qquad (1)$$

n number of analyzed geochemical standards, Y measured elemental level, X declared elemental level in standard material

$$RPD = \frac{200}{n} \cdot \sum_{i=1}^{n} \frac{X_i - Y_i}{X_i + Y_i} \qquad (2)$$

n number of double analyses, X first measured elemental level, Y second measured elemental level

Data processing

Nonparametric statistics (median, minimum, maximum values and percentiles) were calculated first. Where a double analysis was made for the purpose of analytical quality control, the actual level was assumed to be the average value of both analyses. While performing statistical calculations, the levels of an element below the detection limits were assumed to be 50% of the detection limit.

One-way nested analysis of variance (nested ANOVA) was calculated on transformed values with the formula $\ln(1 + C)$, where C represents the elemental level. This transformation was used to assure normal or close to normal distribution of data. Those elements where more than 30% of analyses were below the detection limit were not included in the ANOVA. Calculation was performed by USGS Statpack software package. The design of the nested ANOVA contained four levels:

- "Macro-level"—represents the different sampling areas, as presented in Table 1;

- "Meso-level"—samples taken within a single "macro-area" but geographically separated from each other by at least 1 km;
- "Time level"—samples taken at the same location but within different years (all samples were taken in warm part of the year between late spring and early autumn); and
- "Micro-level"—two or more samples taken at the same sampling point at the same time (for example, on two different sides of the same parking area).

The next statistical analysis contains the comparison of percentile values of major and trace elemental levels in different groups of SD samples, to quantitatively define how anthropogenic or natural factors influence the distribution of major and trace element levels in SD. This was done by dividing the whole set of chemical analysis into two groups for each of the factor of interest separately. Percentile values of samples from each of the group were calculated and compared between each other. Six different separations were made according to six different criteria, as presented in Table 2.

It needed to be noted that 10-km-radius criteria (Table 2) was taken as the measure of proximity since past studies show that smelters can influence dust composition up to 10–15 km away from the source (Žibret and Šajn 2008). The ratio between two percentile values ($RT = P_{\text{influential area}}/P_{\text{non-influential area}}$) was used to numerically evaluate changes in distribution between two groups. For comparing natural factors (carbonates, Bohemian Massif, Permian rocks), the 25th percentile values were used to calculate RT factor. 25th percentile for comparing the distributions of natural factors was selected because it is expected according to the sampling schemes used that this value is not influenced by anthropogenic activities in larger extents. The 75th percentile was used to calculate the RT value for areal sources of dust, such as coal mining and urbanization, and 90th percentile was used in the case of point sources of pollution, such as metallurgical industry, where an exponential decrease in metal levels with increasing distance from a plant is expected (Žibret and Šajn 2008).

Table 2 Separation of the SD samples into groups for the evaluation of the impact of anthropogenic and natural factors on the SD composition

Criteria	Type	Factor description	The first group	The second group
COAL	Anthropogenic impact	The impact of coal mining and coal-firing power plants on the SD composition	201 SD samples, collected in the vicinity (< 10 km) from the nearest open-pit coal mine or coal-firing power plant	105 SD samples, collected far away (> 10 km) from the nearest open-pit coal mine or coal-firing power plant
MET	Anthropogenic impact	The impact of metallurgical industries (ironworks, smelters, metal casting, etc.) on the SD composition	60 SD samples, collected in the proximity (< 10 km) of metallurgical industry	246 SD samples, collected far away (> 10 km) from the metallurgical industry
URB	Anthropogenic impact	The impact of urbanization on the SD composition	90 SD samples, collected in densely urbanized areas (> 50 000 inhabitants)	216 SD samples, collected in rural areas
CARB	Natural impact	The impact of geological composition (carbonate rocks) on the SD composition	48 SD samples taken on the carbonate rocks of the Southern Alps and northern Dinarides	258 SD samples, collected on non-carbonate rocks
SOK	Natural impact	The impact of geological composition (rocks of the Bohemian Massif) on the SD composition	113 SD samples taken on the Bohemian Massif of the Czech Republic	193 SD samples, collected on other rock types
WIT	Natural impact	The impact of geological composition (clastic Permian rocks with coal layers of the Ecca Group) on the SD composition	137 SD samples taken on the Ecca Group of Permian age in the Republic of the South Africa	169 SD samples, collected on other rock types

Table 3 Descriptive statistical parameters for major, minor and trace elemental levels in all SD samples used in this study from all areas

El	Unit	Min	P5	P25	P50	Avg	P75	P95	Max	Std	N	RPD	%R	BLN	DL
Ag	mg/kg	< 0.1	< 0.1	< 0.1	**0.20**	0.47	0.40	1.30	14.7	1.41	306	30	105	0	0.1
Al	mg/kg	0.23	1.06	2.92	**4.28**	3.99	5.21	6.04	6.85	1.58	306	3	104	0.015	0.01%
As	mg/kg	< 1	3.62	7.00	**10.0**	12.8	17.0	30.0	42.0	8.32	306	11.5	154.5	0.165	1
Au	mg/kg	0.0017	0.05	0.05	**0.05**	0.11	0.05	0.18	11.1	0.667	281	8	N/A	0	0.001
Ba	mg/kg	29	126	264	**425**	414	548	635	1837	201	306	4.5	102.5	0.5	1
Be	mg/kg	< 1	< 1	1.0	**2.0**	2.7	4.0	7.0	12	2.17	291	40	N/A	0	1
Bi	mg/kg	< 0.1	0.20	0.30	**0.60**	0.82	1.00	2.50	6.00	0.737	306	20	N/A	0	0.1
Ca	%	0.09	0.29	0.82	**4.21**	5.42	6.36	18.5	22.0	5.89	306	3	103.5	0.005	0.01%
Cd	mg/kg	< 0.1	< 0.1	0.20	**0.40**	0.59	0.70	1.78	7.20	0.728	306	34	104	0	0.1
Ce	mg/kg	16	34	84	**113**	110	136	174	297	43.1	263	5.5	102	0	1
Co	mg/kg	2.5	4.0	16.2	**26.2**	26.6	38.2	49.0	75.5	14.3	306	4.5	113.5	0	0.2
Cr	mg/kg	14.5	46.3	138	**240**	1615	1262	7328	43,050	3992	306	7.5	102.5	0.75	1
Cu	mg/kg	13.8	37.2	59.6	**107**	121	168	244	524	71.8	306	11	106	0.135	0.1
Fe	%	0.79	1.44	4.22	**5.91**	5.67	7.00	9.01	18.5	2.49	306	3	106.5	0	0.01%
Hf	mg/kg	0.50	1.41	3.50	**5.10**	4.90	6.30	7.39	11.0	1.82	263	8	100	0	0.1
Hg	mg/kg	< 0.01	0.02	0.05	**0.09**	0.30	0.19	1.29	6.36	0.748	214	21.5	117.5	0	0.01
In	mg/kg	< 0.05	< 0.05	< 0.05	**0.058**	0.056	0.070	0.110	0.290	0.0364	189	34	N/A	0	0.05
K	%	0.03	0.12	0.40	**0.70**	0.70	0.97	1.26	2.14	0.359	306	1.5	93.5	0	0.01%
La	mg/kg	3.0	6.6	22.7	**34.7**	44.0	67.0	87.7	169	28.6	306	5	116.5	0	0.1
Li	mg/kg	6.30	10.8	16.6	**26.6**	32.1	43.4	66.8	116	19.6	263	5	93.5	0.01	0.1%
Mg	%	0.09	0.23	0.53	**2.10**	2.11	3.09	5.63	8.94	1.73	306	2.5	101.5	0	0.01%
Mn	mg/kg	197	339	919	**1176**	1362	1432	2778	20,000	1379	306	4	103.5	1	1
Mo	mg/kg	0.70	1.40	2.50	**3.30**	4.64	4.90	9.26	104	7.01	306	9.5	106	0	0.1
Na	%	0.002	0.03	0.11	**0.32**	0.51	0.95	1.22	1.56	0.439	306	3.5	98.5	0	0.001%
Nb	mg/kg	1.00	2.85	10.0	**14.6**	32.7	62.0	78.6	122	29.4	291	6	97	0	0.1
Ni	mg/kg	9.8	20.3	43.4	**67.1**	83.2	91.6	191	1148	87.4	306	9.5	112	0.065	0.1
P	%	0.011	0.025	0.038	**0.058**	0.108	0.196	0.243	0.369	0.0852	306	4.5	97	0	0.001%
Pb	mg/kg	10.8	27.1	39.9	**57.3**	104	100	381	835	123	306	12.5	106.5	0.285	0.1
Rb	mg/kg	7.80	18.3	31.5	**53.6**	55.8	76.9	105	184	29.5	263	3	100	0.125	0.1
Re	mg/kg	< 0.005	< 0.005	< 0.005	**< 0.005**	< 0.005	< 0.005	0.006	0.021	0.00169	189	38	N/A	0	0.005
S	%	0.03	0.05	0.05	**0.10**	0.30	0.20	0.50	11.00	1.10	281	27	74	0	0.1%
Sb	mg/kg	0.30	0.80	1.85	**3.30**	4.55	6.60	11.0	25.4	3.72	301	7.5	122.5	0	0.1
Sc	mg/kg	0.60	3.00	7.00	**11.0**	11.3	16.5	20.4	26.0	5.94	306	4	96	0	1

Table 3 continued

El	Unit	Min	P5	P25	P50	Avg	P75	P95	Max	Std	N	RPD	%R	BLN	DL
Se	mg/kg	< 0.5	< 0.5	0.50	**0.50**	0.74	0.55	2.00	4.00	0.616	203	44	N/A	0	0.5
Sn	mg/kg	1.60	2.60	4.90	**8.70**	10.3	13.7	22.2	95.4	8.90	291	22.5	99	0	0.1
Sr	mg/kg	14.0	40.2	78.0	**126**	210	374	476	592	161	306	4.5	99	0	1
Ta	mg/kg	0.20	0.31	0.70	**1.00**	2.30	4.10	5.15	7.30	1.89	263	13.5	112.5	0	0.1
Te	mg/kg	< 0.5	< 0.5	< 0.5	**< 0.5**	0.49	< 0.5	1.82	6.40	0.828	189	39	N/A	0	0.5
Th	mg/kg	0.5	2.0	10.0	**15.2**	15.3	19.5	30.6	69.6	9.06	306	9.5	109.5	0	0.1
Ti	%	0.01	0.11	0.45	**0.83**	0.99	1.53	2.17	4.50	0.691	306	4	103	0	0.001%
Tl	mg/kg	0.05	0.11	0.25	**0.25**	0.34	0.46	0.70	1.20	0.194	203	5	N/A	0	0.05
U	mg/kg	0.1	0.7	2.8	**3.8**	4.5	5.4	10.0	23.6	3.17	281	11.5	96.5	0	0.1
V	mg/kg	4	17	121	**198**	228	270	402	4410	302	306	4.5	112	1.165	1
W	mg/kg	< 0.1	0.60	1.10	**2.00**	3.58	4.70	9.56	63.9	5.41	306	15.5	86.5	0	0.1
Y	mg/kg	5.50	8.00	15.4	**20.2**	19.7	24.2	30.9	45.8	6.78	291	7	108.5	0.01	0.1
Zn	mg/kg	29.0	70.6	153	**259**	323	350	839	2315	310	306	5.5	97.5	0.165	1
Zr	mg/kg	12.0	14.0	113	**162**	163	228	276	400	81.7	291	7.5	100	0.11	0.1

el element, *Min* minimum value, *P5* 5th percentile, *P25* 25th percentile, *P50* median value (in bold letters, to highlight them), *Avg* average value, *P75* 75th percentile, *P95* 95th percentile, *Max* maximum value, *Std* standard deviation, *N* number of analyses, *RPD* average relative percent difference of double analyses, *%R* average recovery of the analysis of geochemical standard materials, *BLN* average values of analysis of triple distilled water, *DL* detection limit, *N/A* not measured or not known

These values could be the first attempt to define average global SD sample

Factor analysis was used to determine geochemical associations in SD and as a secondary indicator of possible sources of elements. It was done on the logarithmically transformed dataset. All 306 samples and 27 elements were included (Ag, Al, As, Ba, Bi, Ca, Cd, Co, Cr, Cu, Fe, K, La, Mg, Mn, Mo, Na, Ni, P, Pb, Sc, Sr, Th, Ti, V, W, Zn). Other elements were excluded because they were not analyzed in all samples or were not loaded in any of the selected factors. The number of factors was determined by the number of eigenvalues having its value above 1. "Varimax raw" factor rotation method was used to determine the matrix of factor loadings in order to increase the variability of factor loadings within each factor. Factor scores were separated into two groups three times ("coal", "metal" and "urban") in the same way it is described in Table 2, and factor score distribution within each group was observed to link factors with certain anthropogenic source. Statsoft Statistica 12 software package was used for factor analysis.

Results and discussion

Table 3 shows the descriptive statistical parameters and quality control parameters for all 47 analyzed elements. The accuracy of the chemical analysis was found to be satisfactory, since the measured recovery rate was found to be between 90 and 120%. Only S and W have recovery rate below 90%, and As and Sb have recovery above 120%. Precision is also satisfactory (RPD is below 20%) for the majority of the elements, except for the Ag, Be, Hg, In, Re, Se, Sn and Te, where RPD is above 20%. The median value of major, minor and trace element levels in < 0.125 mm fraction of SD increase in the following order: Au < In < Hg < Ag < Tl < Cd < Se < Bi < Ta < Be < W < Mo < Sb < U < Al < Hf < Sn < As < Sc < Nb < Th < Y < Co < Li < La < Rb < Pb < Ni < Cu < Ce < Sr < Zr < V < Cr < Zn < Ba < P < S < Mn < Na < K < Ti < Mg < Ca < Fe. Re and Te are not included in this list since their median values were below the detection limit.

Table 4 shows the results of the one-way nested analysis of variance. The largest variance components for most of the elements are observed on hierarchical level 1—the macro-level. This means that SD composition varies the most between different macro-

Table 4 Results of the one-way nested analysis of variance, shown as the percentage (%) of the variance loaded on a specific hierarchical level for a specific element

El	Macro	Meso	Temp	Micro
Ag	29*	49	0	22
Al	81*	15	0	4
As	61*	0	29	10
Ba	58*	15	19	7
Bi	77*	12	0	11
Ca	95*	1	2	1
Cd	69*	0	23	8
Co	85*	11	1	3
Cr	73*	21	0	6
Cu	61*	22	0	16
Fe	72*	24	0	4
Hg	12*	52*	0	37
K	56*	32	0	12
La	90*	1	7*	2
Mg	90*	0	7	3
Mn	51*	38	4	7
Mo	26*	62*	0	11
Na	88*	9*	0	2
Ni	28*	44	14	14
P	89*	9	0	3
Pb	64*	6	22	7
Sc	88*	5	4	3
Sr	83*	16	0	2
Th	86*	4	7	4
Ti	78*	18*	0	4
U	82*	13	0	5
V	76*	16	0	8
W	67*	28	0	5
Zn	36*	0	53*	11
AVG	67	18	7	8

El element, *Macro* macro-level (samples taken in different geographical areas), *Meso* meso-level (samples taken within the same geographical area but separated from each other by at least 500 m), *Temp* temporal level (samples taken in the same place but in a different year), *Micro* micro-level (samples taken during the same time period and at the same sampling point, but separated by 10–20 m)

*Significance on confidential level $q = 0.05$

areas (countries). This is especially evident for the Al, Bi, Ca, Cd, Co, La, Mg, Na, P, Sc, Sr, Th, Ti, U and V, where more than 75% of total variance can be attributed to the macro-scale variations, as a result of regional lithological variations, distances from the sea
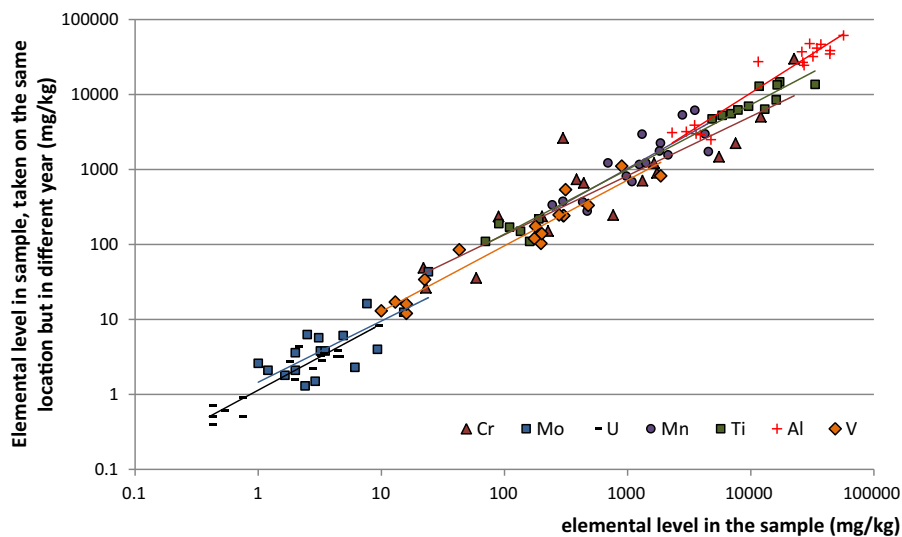
Fig. 2 Scatter plot of the selected elemental levels in SD samples collected at the same locations but in different years (17 data points)

or similar. This result is in agreement with the study of Pingitore et al. (2009) and Gunawardana et al. (2012) which discovered that the most common natural source of road dust particles are erosion of nearby soil and rock. Ca, Mg and Sr enrichments are typical for carbonates, La, Th, U and Al for continental crust and granites and Co, Ti and V for mafic igneous rocks (Parker, 1967), so variations of these elements could be explained with the variations in lithological composition of the areas. Another possible regional source of variations within this group is sea spray deposition near coastlines, contributing to variations of Na and variations in vegetation cover, which could impact the levels of P (Amato et al. 2009).

Increased variance component on level 2—same macro-area but different sampling points—has been measured for Mo, Hg, Ag, Ni, Mn and K. This variance can be caused by larger point source emissions of atmospheric particles, like dust emissions from power plants (K, Hg, Ag) or metallurgical industry (Mo, Ni, Mn; Žibret et al. 2013). Temporal variations for the majority of the elements is low (Table 4), meaning that SD composition on certain point is more or less uniform through time. Figure 2 shows scaling of Cr, Mo, U, Mn, Ti, Al and V levels for samples, which were collected in the same place, but in different time where some samples were taken more than a decade apart. Log–log linear correlation is observed for majority of the elements with correlation

coefficients between 0.67 and 0.94. All log–log regression lines have more or less similar angle. This shows that street dust can be regarded as stable sampling medium, not subjected to quick and rapid temporal changes in its composition. However, Zn, As, Cd, Pb, Ba and Ni have slightly higher temporal variations as other elements (Table 4). Because these elements (except for As) can be linked to emissions from traffic (Adachi and Tainosho 2004; Amato et al. 2011), it could mean that impacts of traffic on SD elemental composition are not constant. Weather changes could also explain increased temporal variations for As or Ba, because some compounds containing both elements are easily soluble in rain water, and are thus washed out in larger amounts during wet seasons. On the microscale (where samples have been collected on the same day, but only few meters apart), only Hg has increased value of level 4 variance component. This can be explained with differences in Hg evaporation as a consequence of local variations in solar insolation. Increased variance component on level 4 is also expressed for Ag, pointing out that the distribution of Ag is subjected to increased local variations.

Table 5 shows the RT values for different influential factors and values of factor loadings from factor analysis. The results from our study show that SD next to the coal mining areas and coal-fired power plants is enriched with Zr, V, Th, Co, Ti, La, U, Sc, Fe, Nb, Mn,

Table 5 Ratio (RT) between two percentile values of the SD composition where 306 SD samples were divided into two groups according to a specific criterion (factor) and the table of factor loadings

Indicator	P75	P90	P75	P25	P25	P25	factor analysis		
Factor	COAL	MET	URB	CARB	SOK	WIT	F1	F2	F3
Ag	0.50	1.38	**2.25**	**4.75**	**4.00**	0.25	− 0.01	**0.78**	− 0.10
Al	**2.41**	0.77	0.95	0.10	**2.41**	1.20	**0.91**	− 0.11	0.14
As	**1.60**	0.51	1.04	0.50	**2.58**	0.71	**0.64**	0.29	0.07
Ba	**1.88**	0.79	1.02	0.45	**2.49**	0.56	**0.68**	0.38	0.16
Be	**2.00**	0.33	1.00	0.50	**5.33**	0.25	N/A	N/A	N/A
Bi	1.33	0.49	**2.94**	0.50	**2.33**	0.40	0.28	**0.67**	0.16
Ca	0.38	1.12	**3.03**	**22.07**	**7.85**	0.05	− 0.11	**0.81**	− 0.43
Cd	0.67	**1.92**	**2.75**	**4.38**	**3.43**	0.13	− 0.23	**0.81**	− 0.20
Ce	**1.75**	0.71	1.01	N/A	**1.94**	0.46	N/A	N/A	N/A
Co	**3.83**	0.95	0.89	0.18	**4.42**	**2.04**	**0.80**	0.00	0.48
Cr	**2.64**	**6.35**	0.91	0.24	0.56	**4.21**	− 0.06	− 0.49	**0.80**
Cu	1.07	0.83	1.18	0.93	**2.98**	0.34	0.32	**0.80**	0.22
Fe	**2.83**	1.21	0.94	0.26	**2.06**	1.40	**0.67**	− 0.06	**0.64**
Hf	1.11	0.88	1.00	N/A	**1.81**	0.53	N/A	N/A	N/A
Hg	1.25	0.40	1.40	1.13	**2.24**	0.36	N/A	N/A	N/A
In	1.00	0.70	1.29	N/A	1.00	1.00	N/A	N/A	N/A
K	**1.58**	0.63	0.80	0.10	**2.47**	0.60	**0.84**	0.08	− 0.03
La	**3.39**	0.42	0.88	0.17	**4.08**	1.39	**0.97**	0.02	0.06
Li	1.36	0.35	1.18	N/A	**2.75**	0.34	N/A	N/A	N/A
Mg	0.63	1.28	**1.62**	**7.74**	**5.90**	0.09	0.01	**0.82**	− 0.33
Mn	**2.66**	**1.97**	0.91	0.31	**1.80**	1.28	0.39	− 0.18	**0.71**
Mo	1.09	**2.19**	**1.69**	1.03	1.22	0.54	− 0.26	**0.69**	0.48
Na	**1.72**	0.29	0.97	0.21	**11.43**	0.11	**0.72**	0.49	− 0.21
Nb	**2.68**	0.23	0.92	0.19	**8.07**	1.11	N/A	N/A	N/A
Ni	**1.98**	**2.31**	0.96	0.40	**1.90**	0.66	0.31	0.35	**0.77**
P	1.19	0.26	0.93	0.82	**5.79**	0.43	**0.75**	0.56	− 0.18
Pb	1.03	**1.67**	**4.70**	**1.53**	0.74	0.89	− 0.49	0.43	0.28
Rb	1.26	0.52	1.05	N/A	**2.81**	0.30	N/A	N/A	N/A
Sb	0.86	0.64	1.48	1.47	**3.08**	0.23	N/A	N/A	N/A
Sc	**3.00**	0.62	0.87	0.13	**3.20**	**1.50**	**0.95**	0.00	0.13
Sn	0.87	0.80	1.18	1.49	**2.96**	0.28	N/A	N/A	N/A
Sr	1.12	0.23	0.88	1.14	**5.67**	0.31	**0.68**	**0.60**	− 0.23
Ta	1.08	0.22	1.10	N/A	**6.33**	0.14	N/A	N/A	N/A
Th	**4.60**	0.63	0.83	0.11	**3.28**	**2.32**	**0.89**	− 0.24	0.19
Ti	**3.66**	0.84	0.88	0.03	**5.83**	2.11	**0.89**	− 0.14	0.23
U	**3.10**	0.47	0.86	0.13	**2.18**	0.60	N/A	N/A	N/A
V	**5.16**	**2.75**	0.90	0.10	**4.04**	**2.48**	**0.70**	− 0.21	0.54
W	1.20	0.47	1.18	0.58	**3.70**	0.40	0.59	0.54	0.19

Table 5 continued

Indicator	P75	P90	P75	P25	P25	P25	factor analysis		
Factor	COAL	MET	URB	CARB	SOK	WIT	F1	F2	F3
Y	**1.96**	0.80	0.97	0.43	**1.86**	0.97	N/A	N/A	N/A
Zn	0.81	**1.96**	**1.76**	**1.81**	**2.23**	0.27	− 0.13	**0.83**	0.09
Zr	**6.99**	0.81	0.97	0.10	**2.33**	**2.76**	N/A	N/A	N/A
	Explained variance by factor analysis (%)						37	26	14

Indicator: percentiles used for calculating the RT value (RT value above 1 means enrichment when a specific criterion is met, while below 1 means depletion; RT values above 1.5 and factor loadings above 0.6 are bolded). COAL, URB, CARB, SOK and WIT—see description in Table 2. F1, F2 and F3—factors 1, 2 and 3. N/A—insufficient data available to present statistically significant results/element was not included in factor analysis. Varimax raw factor rotation was applied for factor analysis

Cr, Al and Be (sorted according to descending *RT* values; *RT* > 2, Table 5). Almost the same set of elements has increased values of factor 1 loadings: La, Sc, Al, Th, Ti, K, Co, P, Na, V, Sr, Ba, Fe and As (sorted in descending order of factor loadings, Table 5). The distributions of factor 1 scores of two groups of samples (Fig. 3) reveal that the first group (near coal mines) has generally higher factor 1 scores than the second one (far from coal mines). The same pattern is evident from the percentile distributions of Al, Co, Fe, La, Sc, Th, Ti, V, Zr and U levels in the samples collected in the vicinity of coal mines and coal-fired power plants and in the samples, collected far away (Fig. 4a). Therefore, a good agreement has been established between different statistical observations. Since Al, Co, Fe, La, Sc, Th, Ti, V, Zr and U also tend to bind within organic matter (Dalwaj 1990), it is reasonable to associate this group of elements with particle emissions from coal mining and coal combustion. Potential sources of dust in such processes are blasting, excavation works, dust emissions from grinding plants, particle remobilization from coal heaps or fly ash storage areas by wind, fly ash emissions from coal-fired power plants and coal transporting by trucks and conveyor belts.

Street dust collected in urbanized areas is, according to RT values, enriched with Pb, Ca, Bi, Cd, Ag, Zn, Mo and Mg (sorted in descending order, Table 5). The similar pattern is observed in factor analysis, because Zn, Mg, Ca, Cd, Cu, Ag, Mo, Bi and Sr (sorted in descending order of factor loading values) are loaded in factor 2. Both results are in good agreement. Figure 3 shows that factor 2 scores are higher in the SD samples, collected in urbanized areas. The same is evident from percentile distributions of Ag, Bi, Ca,

Cd, Mg, Mo, Pb and Zn (Fig. 4b) since samples taken in urbanized areas have higher 25th and 75th percentile values and medians than those of samples taken from and rural areas. It is interesting that Pb is not loaded in factor 2, so factor analysis excludes it from group of elements where their enrichment is typical for urbanization. Factor analysis rather shows that Pb is weakly negatively loaded in factor 1 (natural association). However, results presented in Table 5 and Fig. 4b clearly indicate that Pb fits into this group. These results are in agreement with many other studies, for instance with the study of Wei and Yang (2010), who reported that SD in densely urbanized areas is enriched with Cr, Ni, Cu, Pb, Zn and Cd, while Acosta et al. (2015) found out that street dust in densely urbanized areas is enriched with Zn, Pb, Cu and Cr, compared to low-density or rural areas. This (current) study also showed that Pb, Zn and Cu are linked to the urbanization, which corresponds well to the findings of Trujillo-González et al. (2016), which found out that Pb, Zn and Cu geo-accumulation index in commercial zones of densely populated cities reach values of 4.9, 2.0 and 2.6, respectively, showing that SD in such zones is highly polluted with Pb, and moderately polluted with Zn and Cu. The enrichment with Ca and Mg can be caused by the particles originating from weathering of construction materials (cement, lime, etc.). The enrichment with Ag in urban areas could be explained by the release of Ag nanoparticles from different sources, since Ag nanoparticles are increasingly used as antibacterial and antifungal agent in many applications (Yu et al. 2013; Ermolin et al. 2017), for example in paints for outdoor facades (Kaegi et al. 2010). The Bi enrichment in SD of the urban environment found in this
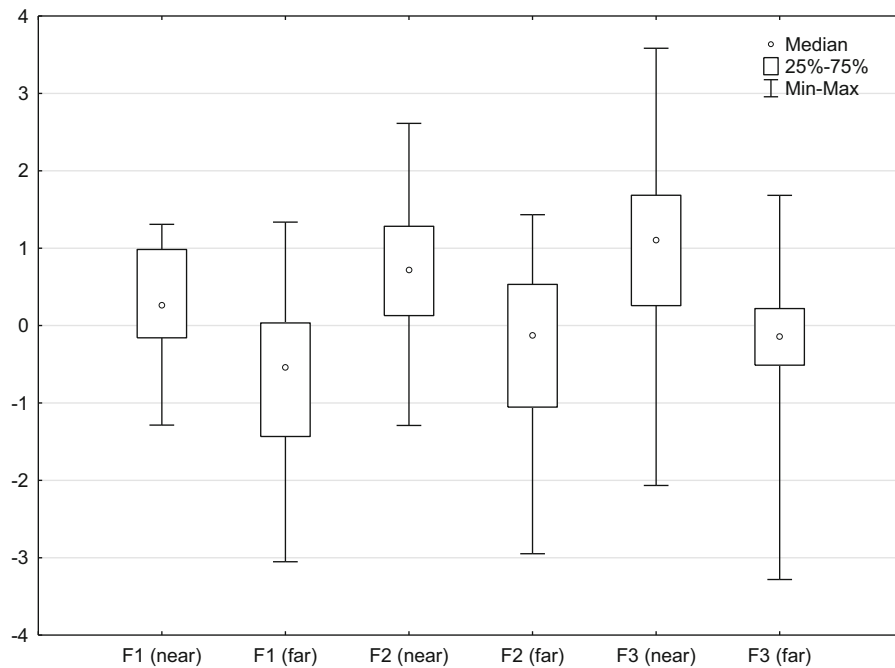
Fig. 3 Comparison of factor scores distributions for different groups of SD samples. The set of factor scores was divided according to the studied anthropogenic impact: factor 1 (F1) according to the distance from coal-firing power plants and coal mines (near: < 10 km; far: > 10 km), factor 2 (F2) according to the urbanization of the area where sample was taken (near: sample taken in urbanized areas of more than 50.000 inhabitants, far: sample taken in small town, villages or rural areas) and factor 3 (F3) according to the distance from metallurgical and smelting plants (near: < 10 km; far: > 10 km)

study could be attributed to the use of Bi in white paints.

The third investigated anthropogenic factor is the impact of metallurgical and smelting plants on the SD composition. *RT* indicator (Table 5) shows that SD in the vicinity of aforementioned plants is enriched with Cr, V, Ni, Mo, Mn, Zn, Cd and Pb (sorted in the descending order). SD samples taken in the vicinity of metallurgical plants are enriched up to six times (the case of Cr enrichment), compared to elemental levels in SD samples, taken far away from such plants. Factor analysis revealed the geochemical association of Cr, Ni, Mn and Fe, which is represented by factor 3. Elevated factor 3 scores are found in SD samples, collected in the vicinity of such plants (Fig. 3). Figure 4c shows the percentile distributions of Cr, V, Ni and Mn levels in samples, taken next to the metallurgical plants and in samples, taken far from them. Enrichment of Cr, V and Ni next to the metallurgical plants is evident. These results are in line with other studies. Li et al. (2013) studied SD

composition around Pb/Zn smelter and detected that emissions from it caused enrichment with Hg, Pb, As and Cu, while Ordóñez et al. (2015) show that Zn–Cd–Hg–Ag–Pb–As enrichment in SD is characteristic for dust emissions from Zn smelter and Fe–Cr–V–Mn enrichment for dust emissions from steel plants. Very similar results were obtained by Šajn (2006), who showed that Cr–Co–Mo–Ni–W anomaly in attic dust can be attributed to dust emissions from metallurgical plants and Ag–As–Cd–Mo–Pb–S–Sb–Sn–Zn anomaly as a result of Pb smelting in the area. In this study, SD samples were taken in the vicinity of many different casting and ironworking plants, as well as around Pb–Zn, ferrochromium and V smelters. Despite the fact that all of these plants could emits wide variety of metals and metalloids, the general trend derived from this study points out that the Cr–Ni–Mn–Fe enrichment in SD is a general characteristics for emissions from metallurgical plants.

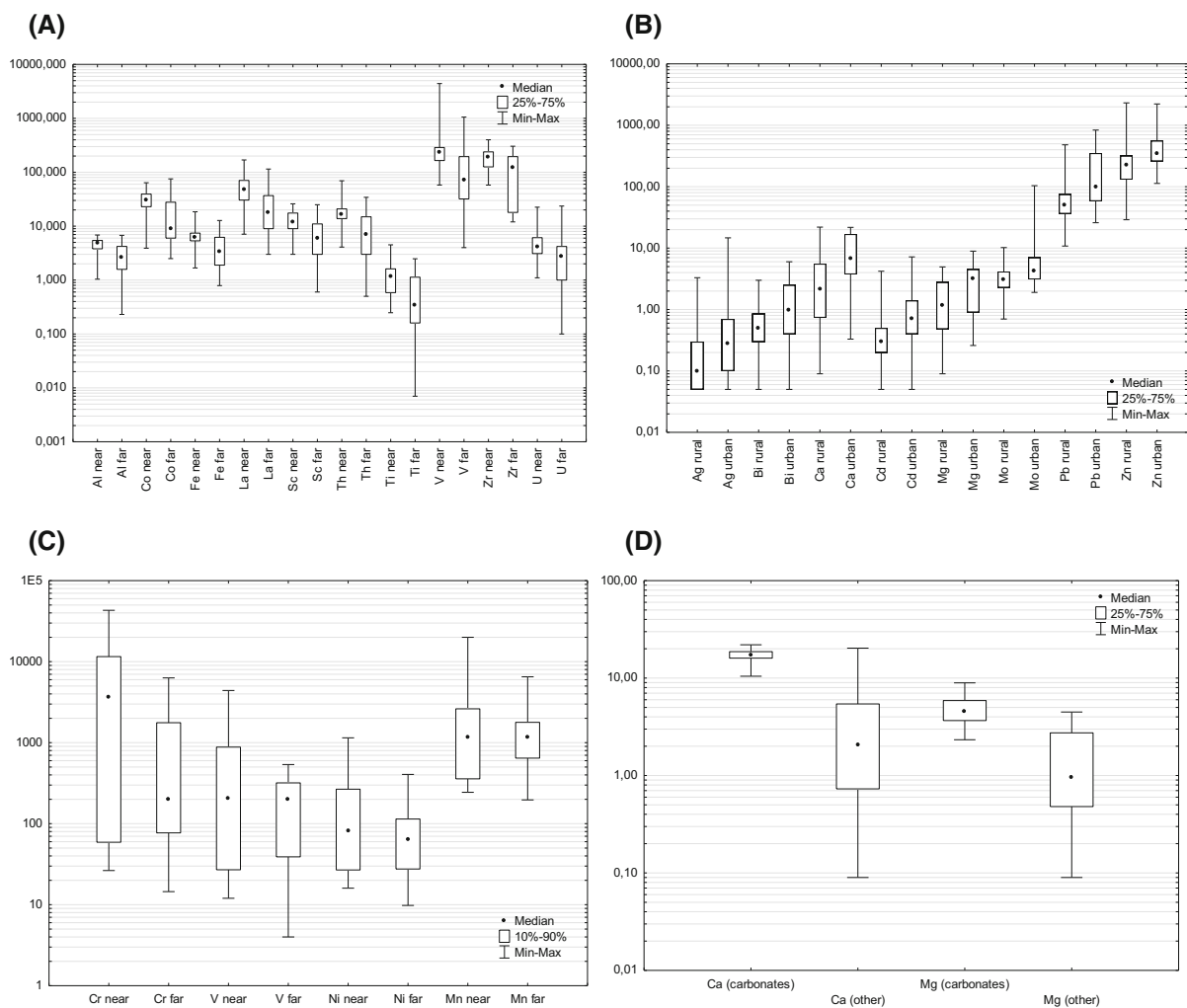The last assessment was how lithology affects the SD elemental composition. The highest recorded

(A)

(B)

(C)

(D)

Fig. 4 Comparison of elemental-level distributions for different groups of SD samples. **a** Distribution of Al, Co, Fe, La, Sc, Th, Ti, V, Zr and U in SD samples, collected near coal mine or coal-fired power plant (< 10 km; 201 samples), and samples, collected far from them (> 10 km; 105 samples). **b** Distribution of Ag, Bi, Ca, Cd, Mg, Mo, Pb and Zn in SD samples, collected in urbanized areas (> 50.000 inhabitants; 90 samples), and SD samples, collected in towns, villages or rural areas (< 50.000 inhabitants, 216 samples). **c** Distribution of Cr, V, Ni and Mn in SD samples, collected near metallurgical or smelting plants (< 10 km; 60 samples), and samples, collected far from them (> 10 km; 216 samples). **d** distribution of Ca and Mg in SD samples, collected on areas composed of carbonates (48 samples), and samples, collected on areas of non-carbonate composition (258 samples). All values are in mg/kg, except for Al, Ti, Ca and Mg, which are shown in %

influence on the SD composition assessed in this study was the influence of carbonates, because *RT* factor for carbonates in the case of Ca and Mg is 22 and 7.74, respectively (Table 5). High impact of carbonates on the Ca and Mg levels in SD is also evident from their percentile distributions in two groups of SD samples (Fig. 4d). This result is in agreement with other studies, which pinpoint that natural sources of particles, such as erosion of soil and rock in SD generally

prevails over anthropogenic ones (Pingitore et al. 2009; Gunawardana et al. 2012). The Ag and Cd enrichments on carbonates could also be attributed to the natural geo-environment typifying Slovenian territory because several sites with polymetallic sulfide mineralization containing these two elements are known, as well as Cd enrichment in soils, developed as weathering residue of carbonates. The SD in the Bohemian Massif, composed of pre-Cambrian and

Paleozoic rocks, alkali igneous intrusions and Neogene deposits containing lignite, is enriched with Na–Nb–Ca–Ta–Mg–Ti–P–Sr–Be, as evident from *RT* factor (Table 5). This can be attributed to the area's highly diverse geological composition, ranging from metamorphic, igneous and sedimentary rocks. High *RT* values in this case, similarly as in the case of carbonates, are recorded, reaching 11 in the case of Na and 8 in the case of Nb. SD collected in the South African pre-Cambrian Kaapvaal Craton, containing intracratonic carboniferous sedimentary rocks, and coal in the eMalahleni area is enriched with Cr–Zr–V–Th–Co. This is possibly the effect of natural enrichment with aforementioned elements in mafic and ultramafic rocks, which commonly occurs in the Kaapvaal Craton (Becker and Le Roex 2006), and possibly also the consequence of numerous heavy industry, presented in the wider area. The results of this study show that natural factors affecting SD composition surpass anthropogenic ones. *RT* values for anthropogenic factors typically reach value between 2 and 7, while *RT* values for natural factors reached values over 20.

Conclusions

Spatial and temporal variations in the chemical composition of SD were assessed by nested analysis of variance, while impact of different natural and anthropogenic factors on elemental levels in SD by calculating enrichment factors and factor analysis. Analysis of variance shows that the largest component of variance of the majority of the elements can be found on the "macro-level" (between countries/continents) scale and can be explained with differences in geological composition. Exceptions are Hg, Mo, Ni and Ag, where the largest component of variance was detected on a level, representing different sampling points within a single sampling area (several kilometers). The variance component, representing temporal factor, is increased for Zn and to a smaller extent also to As, Cd and Pb. On the "micro-level" (several meters), elevated variance component values were detected for Hg and Ag. Enrichments of up to 20 times are characteristic for natural (geo-genic) influential factors, while enrichments up to seven times for anthropogenic ones. The chemical footprint of coal mining and coal-fired power production to the SD

composition is the enrichment with Al–Co–Fe–La–Sc–Th–Ti–V–Zr–U, while the characteristic footprint of metallurgical activities is the enrichment with Cr–V–Ni–Mn. The increased levels of Ag–Bi–Ca–Cd–Mg–Mo–Pb–Zn are signs of contamination caused by urbanization. Besides obtaining statistical patterns of SD composition on large dataset and on samples, taken far apart, the results of this study also stress out the importance of considering natural factors first and only then anthropogenic ones when interpreting geospatial distribution of elements in SD. This study is also the first attempt to establish global average composition of SD.

References

Acosta, J. A., Gabarrón, M., Faz, A., Martínez-Martínez, S., Zornoza, R., & Arocena, J. M. (2015). Influence of population density on the concentration and speciation of metals in the soil and street dust from urban areas. *Chemosphere, 134,* 328–337.

Adachi, K., & Tainosho, Y. (2004). Characterization of heavy metal particles embedded in tire dust. *Environment International, 30,* 1009–1017.

Adriano, D. C. (1986). *Trace elements in the terrestrial environments.* Berlin: Springer.

Al-Khashman, O. A. (2007). Determination of metal accumulation in deposited street dusts in Amman, Jordan. *Environmental Geochemistry and Health, 29,* 1–10.

Amato, F., Alastuey, A., de la Rosa, J., Gonzalez Castanedo, Y., Sánchez de la Campa, A. M., Pandolfi, M., et al. (2014). Trends of road dust emissions contributions on ambient air particulate levels at rural, urban and industrial sites in southern Spain. *Atmospheric Chemistry and Physics, 14,* 3533–3544.

Amato, F., Pandolfi, M., Moreno, T., Furger, M., Pey, J., Alastuey, A., et al. (2011). Sources and variability of inhalable road dust particles in three European cities. *Atmospheric Environment, 45,* 6777–6787.

Amato, F., Pandolfi, M., Viana, M., Querol, X., Alastuey, A., & Moreno, T. (2009). Spatial and chemical patterns of PM10 in road dust deposited in urban environment. *Atmospheric Environment, 43,* 1650–1659.

Barandovski, L., Cekova, M., Frontasyeva, M. V., Pavlov, S. S., Stafilov, T., Steinnes, E., et al. (2008). Atmospheric deposition of trace element pollutants in Macedonia studied by the moss biomonitoring technique. *Environmental Monitoring and Assessment, 138,* 107–118.

Bavec, Š. (2015). Geochemical investigations of potentially toxic trace elements in urban sediments of Idrija. *Geologija, 58,* 111–120. https://doi.org/10.5474/geologija.2015.009.

Bavec, Š., Biester, H., & Gosar, M. (2014). Urban sediment contamination in a former Hg mining district, Idrija, Slovenia. *Environmental Geochemistry and Health, 36,* 427–439.

Becker, M., & Le Roex, A. P. (2006). Geochemistry of South African on- and off-craton, Group I and Group II kimberlites: Petrogenesis and source region evolution. *Journal of Petrology, 47,* 673–703.

Bernabe, J. M., Carretero, M. I., & Galan, E. (2005). Mineralogy and origin of atmospheric particles in the industrial area of Huelva (SW Spain). *Atmospheric Environment, 39,* 6777–6789.

Charlesworth, S., Everett, M., McCarthy, R., Ordóñez, A., & de Miguel, E. (2003). A comparative study of heavy metal concentration and distribution in deposited street dusts in a large and a small urban area: Birmingham and Coventry, West Midlands, UK. *Environment International, 29,* 563–573.

Dalwaj, J. S. (1990). *Trace elements in coal.* Butterworths London, Boston, Singapore, Sydney, Toronto: Wellington.

Duong, T. T. T., & Lee, B. K. (2009). Partitioning and mobility behavior of metals in road dusts from national-scale industrial areas in Korea. *Atmospheric Environment, 43,* 3502–3509.

Ermolin, M. S., Fedotov, P. S., Ivaneev, A., & Karandashev, V. K. (2017). Isolation and quantitative analysis of road dust nanoparticles. *Journal of Analytical Chemistry, 75,* 520–532.

Gosar, M., Šajn, R., & Teršič, T. (2016). Distribution pattern of mercury in the Slovenian soil: Geochemical mapping based on multiple geochemical datasets. *Journal of Geochemical Exploration, 167,* 38–48.

Gunawardana, C., Goonetilleke, A., Egodawatta, P., Dawes, L., & Kokot, S. (2012). Source characterisation of road dust based on chemical and mineralogical composition. *Chemosphere, 87,* 163–170.

Harmens, H., Norris, D. A., Steinnes, E., Kubin, E., Piispanen, J., Alber, R., et al. (2010). Mosses as biomonitors of atmospheric heavy metal deposition: Spatial patterns and temporal trends in Europe. *Environmental Pollution, 158,* 3144–3156.

Herngren, L., Goonetilleke, A., & Ayoko, G. A. (2006). Analysis of heavy metals in road-deposited sediments. *Analytica Chimica Acta, 571,* 270–278.

Kaegi, R., Sinnet, B., Zuleeg, S., Hagendorfer, H., Mueller, E., Vonbank, R., et al. (2010). Release of silver nanoparticles from outdoor facades. *Environmental Pollution, 158,* 2900–2905.

Kemppainen, S., Tervahattu, H., & Kikuchi, R. (2003). Distribution of airborne particles from multi-emission source. *Environmental Monitoring and Assessment, 85,* 99–113.

Lanzerstorfer, C., & Logiewa, A. (2018). The upper size limit of the dust samples in road dust studies: Benefits of a combined sieving and air classification sample preparation procedure. Environmental Pollution, accepted manuscript. https://doi.org/10.1016/j.envpol.2018.10.131. **(in press)**

Li, Z., Feng, X., Li, G., Bi, X., Zhu, J., Qin, H., et al. (2013). Distributions, sources and pollution status of 17 trace metal/metalloids in the street dust of a heavily industrialized city of central China. *Environmental Pollution, 182,* 408–416.

Li, Y., Yu, Y., Yang, Z., Shen, Z., Wang, X., & Cai, Y. (2016). A comparison of metal distribution in surface dust and soil among super city, town, and rural area. *Environmental Science and Pollution Research, 23,* 7849–7860.

Manno, E., Varrica, D., & Dongarrá, G. (2006). Metal distribution in road dust samples collected in an urban area close to a petrochemical plant at Gela, Sicily. *Atmospheric Environment, 40,* 5929–5941.

McQueen, A. D., Johnson, B. M., Rodgers, J. H., Jr., & English, W. R. (2010). Campus parking lot stormwater runoff: Physicochemical analyses and toxicity tests using *Ceriodaphnia dubia* and *Pimephales promelas. Chemosphere, 79,* 561–569.

Miler, M., & Gosar, M. (2015). Chemical and morphological characteristics of solid metal-bearing phases deposited in snow and stream sediment as indicators of their origin. *Environmental Science and Pollution Research, 22,* 1906–1918.

Ordóñez, A., Álvarez, R., De Miguel, E., & Charlesworth, S. (2015). Spatial and temporal variations of trace element distribution in soils and street dust of an industrial town in NW Spain: 15 years of study. *Science of the Total Environment, 524–525,* 93–103.

Parker, R. L. (1967). *Data on geochemistry, 6th edition. Chapter D. Composition of the Earth's crust.* USGS, Geological Survey Professional paper 440-D.

Piña, A. A., Torres, G. V., Monroy, M. F., Luszczewski, A. K., & Leyva, R. R. (2000). Scanning electron microscope and statistical analysis of suspended heavy metal particles in San Luis Potosi, Mexico. *Atmospheric Environment, 34,* 4103–4112.

Pingitore, N. E., Jr., Clague, J. W., Amaya, M. A., Maciejewska, B., & Reynoso, J. J. (2009). Urban airborne lead: X-ray absorption spectroscopy establishes soil as dominant source. *PLoS ONE, 9,* 99. https://doi.org/10.1371/journal.pone.0005019.

Prichard, H. M., Sampson, J., & Jackson, M. (2009). A further discussion of the factors controlling the distribution of Pt, Pd, Rh and Au in road dust, gullies, road sweeper and gully flusher sediment in the city of Sheffield, UK. *Science of the Total Environment, 407,* 1715–1725.

Šajn, R. (1999). *Geochemical properties of urban sediments on the territory of Slovenia.* Ljubljana: Geological Survey of Slovenia.

Šajn, R. (2005). Using attic dust and soil for the separation of anthropogenic and geogenic elemental distributions in an old metallurgic area (Celje, Slovenia). *Geochemistry: Exploration, Environment, Analysis, 5,* 59–67.

Šajn, R. (2006). Factor analysis of soil and attic-dust to separate mining and metallurgy influence, Meza Valley, Slovenia. *Mathematical Geology, 38,* 735–747.

Salminen, R., Batista, M. J., Bidovec, M., Demetriades, A., De Vivo, B., De Vos, W., et al. (2005). *Geochemical atlas of Europe*. Espoo: Geological Survey of Finland.

Shi, G., Chen, Z., Bi, C., Wang, L., Teng, J., Li, Y., et al. (2011). A comparative study of health risk of potentially toxic metals in urban and suburban road dust in the most populated city of China. *Atmospheric Environment, 45,* 764–771.

Tokalıoğlu, Ş., & Kartal, Ş. (2006). Multivariate analysis of the data and speciation of heavy metals in street dust samples from the Organized Industrial District in Kayseri (Turkey). *Atmospheric Environment, 40,* 2797–2805.

Trujillo-González, J. M., Torres-Mora, M. A., Keesstra, S., Brevik, E. C., & Jiménez-Ballesta, R. (2016). Heavy metal accumulation related to population density in road dust samples taken from urban sites under different land uses. *Science of the Total Environment, 553,* 636–642.

Vaze, J., & Chiew, F. H. S. (2002). Experimental study of pollutant accumulation on an urban road surface. *Urban Water, 4,* 379–389.

Venturini, E., Vassura, I., Raffo, S., Ferroni, L., Bernardi, E., & Passarini, F. (2014). Source apportionment and location by selective wind sampling and Positive Matrix Factorization. *Environmental Science and Pollution Research, 21,* 11634–11648.

Wang, W. H., Wong, M. H., Leharne, S., & Fisher, B. (1998). Fractionation and biotoxicity of heavy metals in urban dusts collected from Hong Kong in London. *Environmental Geochemistry and Health, 20,* 185–198.

Watanabe, H., Nakajima, F., Kasuga, I., & Furumai, H. (2011). Toxicity evaluation of road dust in the runoff process using a benthic ostracod Heterocypris incongruens. *Science of the Total Environment, 409,* 2366–2372.

Wei, X., Gao, B., Wang, P., Zhou, H., & Lu, J. (2015). Pollution characteristics and health risk assessment of heavy metals in street dusts from different functional areas in Beijing, China. *Ecotoxicology and Environmental Safety, 112,* 186–192.

Wei, B., & Yang, L. (2010). A review of heavy metal contaminations in urban soils, urban road dusts and agricultural soils from China. *Microchemical Journal, 94,* 99–107.

Whiteley, J. D., & Murray, F. (2003). Anthropogenic platinum group element (Pt, Pd and Rh) concentrations in road dusts and roadside soils from Perth, Western Australia. *Science of the Total Environment, 317,* 121–135.

Yu, S., Yin, Y., & Liu, J. (2013). Silver nanoparticles in the environment. *Environmental Science: Processes & Impacts, 15,* 78–92.

Zheng, N., Liu, J., Wang, Q., & Liang, Z. (2010). Health risk assessment of heavy metal exposure to street dust in the zinc smelting district, Northeast of China. *Science of the Total Environment, 408,* 726–733.

Žibret, G. (2012). Impact of dust filter installation in ironworks and construction on brownfield area on the toxic metal concentration in street and house dust (Celje, Slovenia). *Ambio, 41,* 292–301.

Žibret, G., & Rokavec, D. (2010). Household dust and street sediment as an indicator of recent heavy metals in atmospheric emissions: A case study on a previously heavily contaminated area. *Environmental Earth Sciences, 61,* 443–453.

Žibret, G., & Šajn, R. (2008). Modelling of atmospheric dispersion of heavy metals in the Celje area, Slovenia. *Journal of Geochemical Exploration, 97,* 29–41.

Žibret, G., Van Tonder, D., & Žibret, L. (2013). Metal content in street dust as a reflection of atmospheric dust emissions from coal power plants, metal smelters, and traffic. *Environmental Science and Pollution Research, 20,* 4455–4468.